doi:10.1038/nature11092

The HARPS spectrograph

The "High Accuracy Radial velocity Planet Searcher" (HARPS) is to date possibly the most precise instrument to detect variations in the radial velocity of astronomical objects [1]. It is installed at ESO's 3.6 m telescope at La Silla Observatory in Chile. The fiber-fed, cross-dispersed echelle spectrograph has a resolution of $R = 115000$ which corresponds to ~ 5 GHz at 500 nm. It covers the wavelength range from 380 to 690 nm in echelle orders 89 through 161. The fiber output facet is imaged on the detector, a mosaic of two 2k $\times$ 4k CCDs. Each extracted pixel can linearly accumulate more than 250000 electrons, allowing for a signal-to-noise ratio (SNR) of 500. The CCDs are arranged with a gap between them, such that one echelle order (number 115, containing 530 to 534 nm) is not recorded.

In order to achieve a high sensitivity to radial velocity variations, several measures were taken to reduce both systematic and statistic uncertainties. An optimal resolution was chosen according to a carefully determined trade-off between the size of instrument, telescope and the input aperture considering typical spectra of solar type stars [25]. Together with the wavelength range this determines the photon noise limited repeatability. According to equation 15 in ref. [2] adapted for the smaller spectral range, the photon noise limited repeatabilty of HARPS computes to

$$\sigma_v^{total} \approx 0.55 \left(\frac{500}{500}\right) \left(\frac{1.5 \times 10^5}{1.15 \times 10^5}\right)^{1.5} \mathrm{cm\,s^{-1}} = 0.8\,\mathrm{cm\,s^{-1}}, \qquad (1)$$

when calibrating the instrument with a single exposure with a frequency comb that has a SNR of 500, a line spacing of 15 GHz and covers the spectrum accessible with HARPS. Although being designed for sub-m s^{-1} repeatability only, HARPS has the potential of detecting shifts on the cm s^{-1} scale, provided that instrumental drifts can be tracked reliably and systematic effects can be reduced to this level.

Obtaining photon noise limited uncertainty of the stellar spectra requires the elimination of all systematic effects at that level. The spectrograph is put in a vacuum vessel, evacuated to below 0.01 mbar and temperature stabilized with a long term stability of the order of a few 10 mK and day-to-day variations of less than 1 mK [15]. The detector is operated at liquid nitrogen temperature with a resulting stability of ± 50 mK. However, not only must the instrument be as stable as possible, but the beam injection to the spectrograph also must not vary. Therefore, the light is coupled to

a multimode fiber, and the position of the star's image at the telescope's focal plane is servo-controlled to always be centered with the fiber's input facet. Additionally, a static double scrambler is installed at the interface to the HARPS vacuum vessel that exchanges the fibers' near and far field. This reduces the residual preservation of an asymmetric illumination of the input facet at the output facet which acts as the spectrograph's input slit.

With these measures and a generally very stable and robust mechanical design, HARPS has a passive stability of better than $1\,\mathrm{m\,s^{-1}}$ over one night [10]. To be able to measure the residual drifts of the spectrograph and to further improve its performance, it is fed by two fibers whose images are separated on the CCD by ≈ 15 pixels in the cross-dispersed direction. In normal operation, one fiber delivers the starlight while the second fiber is continuously fed with calibration light. Any global drift of the instrument is monitored and can be subtracted from the data. With this simultaneous calibration scheme it could be shown that the spectrograph's average drift is of the order of $10\,\mathrm{cm\,s^{-1}}$ during approximately a day and a repeatability of $24\,\mathrm{cm\,s^{-1}}$ is feasible, using a thorium lamp for calibration [1].

The frequency comb system

A laser frequency comb (LFC) is formed by a pulsed femtosecond laser that emits light at many frequencies (up to 10^6 lines). The frequency difference between two neighboring lines corresponds to the repetition frequency f_{rep} of the pulsed laser and is therefore constant across the comb spectrum. The frequency f_n of each line is characterized by a unique integer n such that $f_n = n f_{rep} + f_0$ with f_0 being the so-called carrier-envelope offset frequency [3]. Since both f_{rep} and f_0 are radio frequencies, they can be stabilized to an atomic clock using well established electronic phase locking techniques. In this way, each optical frequency obtains the accuracy and long-term stability of the atomic clock.

While there are several frequency comb systems proposed to match the criteria for a spectrograph calibrator [4,5,7,26,27], our choice is to use a fiber-laser-based LFC. Fiber lasers are technically mature and turn-key systems — including complex wavelength conversions — are commercially available. When using Yb-fiber lasers, high-power amplifiers can be employed and the second harmonic of the central wavelength ($\approx 1030\,\mathrm{nm}$) is in center of the desired wavelength range. This laser system therefore fulfills the most impor-

tant prerequisites. However, the required fiber length limits the round-trip time in the oscillator and thus the line spacing of the laser (its pulse repetition rate) is currently limited to roughly below 1 GHz [28]. Fabry-Pérot cavities (FPCs) acting as periodic, high resolution spectral filters can be implemented to increase the line spacing [2]. Since fiber lasers are operating in the infrared regime — while most high precision spectrographs cover the visible spectrum — the comb's spectrum must be transformed via nonlinear frequency conversion processes (sum frequency generation and spectral broadening). The challenge is to combine the frequency conversion and the high pulse repetition rate. A high repetition rate corresponds to low pulse energies that are detrimental for nonlinear conversion processes. Filtering the lines of a broad spectrum, however, suffers from the dispersion of the FPC mirrors. See [5]for a detailed discussion. Our approach to overcome this dilemma employs two key components. First, a comb system based on an Yb-fiber laser enables the use of Yb-fiber high-power amplifiers to reduce the problem of low pulse energies. Second, when using specially designed photonic crystal fibers (PCFs), relatively low pulse energies are sufficient to obtain sufficient spectral broadening [24].

Our frequency comb system to calibrate the HARPS spectrograph is based on a commercial Yb-fiber oscillator (Menlosystems Orange Comb 250) with a repetition rate of $f_{rep} = 250\,\mathrm{MHz}$. The laser is operated in the dispersion-managed regime, giving a spectral bandwidth of $\approx 50\,\mathrm{nm}$ centered around 1050 nm. The fourth harmonic of the repetition rate is phase-locked at 1 GHz to a low noise RF synthesizer, which is referenced to a rubidium atomic clock. The clock has a stability of approximately 10^{-11} per month (6 kHz at a wavelength of 500 nm or $0.3\,\mathrm{cm\,s^{-1}}$ Doppler shift). Before traveling to La Silla the absolute frequency of the clock was measured against a GPS disciplined hydrogen maser with an uncertainty on the 10^{-11} level. To guarantee long-term stability at the telescope, regular on site calibration of the clock with a simple GPS receiver will be sufficient. The offset frequency, detected with a f-$2f$ interferometer [3], is locked at 20 MHz to another synthesizer which is referenced to the rubidium clock as well. The line numbers n of the filtered comb lines are determined by a comparison with a thorium spectrum lamp via HARPS. For this application the uncertainty in the absolute frequencies of the thorium lines of typically less than 100 MHz is sufficient.

Several FPCs in series are employed to increase the line spacing in order to resolve the comb lines with the spectrograph. Neglecting dispersion and

the Guoy phase they have a transmission maximum every free spectral range (FSR= $c/2L$) and when the cavity length is matched to the m-th fraction of the length of the comb generator, only every m-th line is transmitted. Group velocity dispersion (GVD) of the mirrors and the medium between the mirrors affects the transmitted spectral bandwidth and induce a shift of the line center when considering the finite linewidth of the comb lines [5]. Thus, low dispersion mirrors must be employed to minimize these effects.

Three or four FPCs in series are tested in our setup to guarantee a sufficient suppression of intermediate lines [22]. The line spacing is increased to 18 GHz which is well resolved by HARPS. The FPCs consist of a plane and a concave mirror of which the plane mirror is mounted on a piezo element to enable changing the distance between the mirrors and thus actively stabilizing the cavity length. The cavity mirrors have a nominal reflectivity of 99.2 %, giving a theoretical finesse of $\mathcal{F} \approx 390$ for all cavities. The first cavity was set to a filter ratio of $m_1 = 9$, and generated a 2.25 GHz line spacing, while the following cavities were set to 18 GHz ($m_{2-4} = 72$). The length of the FPC is stabilized with an additional continous wave (cw) laser. This external cavity diode laser is locked onto one line of the comb with zero frequency offset. Its light is split up and spatially overlapped with the comb light directly in front of the FPCs with a polarizing beamsplitter cube. The cw laser is phase modulated with a few MHz and the FPCs are stabilized to it via a modified Pound-Drewer-Hall locking scheme [23] used in transmission. Long term drifts of the FPCs can be compensated by thermally tuning the FPC mount. With a wavemeter with a stability and resolution of 10 MHz the cw laser is permanently monitored to ensure that always the same comb lines are transmitted through the FPCs.

Since each of the FPCs transmits on every m-th line the corresponding loss of average power needs to be compensated. An optical fiber amplifier is readily realized with a few cm of core-pumped Yb fiber to deliver up to 500 mW average power. We use such an amplifier after each FPC. After the last FPC a double-clad Yb-fiber amplifier is employed that can deliver average powers up to 10 W to facilitate the subsequent nonlinear processes. The spectral bandwidth after these amplifiers suffers from reabsorption and gain narrowing. The initially 50 nm wide spectrum reduces to a 3 dB bandwidth of only 20 nm after the high-power amplifier.

The spectral bandwidth of HARPS covers 380-690 nm and therefore the light from the Yb-fiber laser operating around 1050 nm must be converted. Short pulses are required to drive nonlinear conversion processes efficiently

and thus a pulse compressor with a prism and grating pair is used to compensate both GVD and third-order dispersion of the fibers. The pulses are compressed to ~ 100 fs which is close to the Fourier-transform limit of 80 fs. The LFC is converted to the green spectral region around 525 nm by second harmonic generation (SHG) in a lithium triborate (LBO) crystal. Strictly speaking, the sum frequencies of all combinations of comb lines are generated but this is commonly termed SHG as well. The resulting spectral width of the green LFC of 5 nm is insufficient for calibrating HARPS. Therefore we use self phase modulation in a highly nonlinear photonic crystal fiber (PCF) for spectral broadening. This fiber was specially developed for this project [24] at the Max-Planck-Institute for the Physics of Light. With pulse energies of only 5 pJ a spectral bandwidth of 140 nm at -20 dB below the peak could be obtained (see figure S1). At this power level the spectrum can be easily flattened with an adaptive filter such as a spatial light modulator that has a typical dynamic range of > 20 dB.

Suppression of intermediate comb lines

Increasing the line spacing of a frequency comb with FPCs will inevitably lead to suppressed, but still existing intermediate lines. Since the suppressed lines are not resolved from the transmitted lines by the spectrograph, any asymmetry in the line distribution will lead to a shift of the detected line center [5]. The frequency and thus position of the fundamental comb lines is known precisely. An important question is thus how well the lines need to be suppressed if there is an asymmetry in their intensities.

In figure S2, the calibration error as a function of the normalized intensity difference $(I_s - I_w)/I_s$ is plotted with I_s and I_w being the intensity of the stronger and weaker neighboring lines at 2.25 GHz respectively. It shows that a normalized intensity difference of only 10^{-5} already leads to a shift of 20 kHz (at a wavelength of 500 nm) if there was no suppression of these unresolved neighboring lines. This shift corresponds to $1\,\mathrm{cm\,s^{-1}}$ Doppler shift. On the other hand, if the weaker neighboring line is completely suppressed (i.e. a normalized intensity difference $= 10^0$), the suppression of the stronger line must be better than 50 dB to ensure that the calibration error is smaller than 20 kHz. A line separation of 2.25 GHz is chosen for demonstration as this is still unresolved by HARPS (which has a resolution of 5 GHz) and thus has a large effect without being detected as a separate line. Moreover, in our

setup, the 2.25 GHz line is the one with least suppression since the first of the three FPCs in our setup has a free spectral range of 2.25 GHz.

With the FPCs, 50 dB suppression are easily achieved for all intermediate lines [7]. The highly nonlinear effects in the PCF, however, can lead to a reamplification of the suppressed lines [6,17,18]. Since these effects are phase and intensity sensitive, the reamplification can be asymmetric with respect to a transmitted line and even vary in time. Thus, if the lines are reamplified to less than 50 dB suppression a shift of the line center on the spectrograph can become detectable.

In our setup with three FPCs, the suppression of the strongest intermediate line (at 2.25 GHz from the transmitted line) theoretically reaches 79 dB as shown in figure S3. In the setup with four FPCs an additional cavity with an FSR of 18 GHz is added. This leads to a theoretical suppression of the strongest intermediate line (at 250 MHz from the transmitted line) of 101 dB.

We have carried out an analysis in which we measured directly the suppression of the intermediate comb lines. A cw laser was phase stabilized to one of the comb lines transmitted by the FPC, frequency doubled and superimposed with the broadened comb on a photodetector. The cw laser emitted light at 1065 nm and had a linewidth of < 100 kHz, i.e. narrower than the comb lines. Since the cw laser was stabilized 20 MHz from a transmitted comb line in the infrared, a strong beat at 40 MHz is observed between the frequency doubled cw laser and the nearest line of the broadened comb (see the inset of figure S4). Using the setup with three FPCs, the beat notes of the cw laser with the strongest suppressed lines (at ± 2.25 GHz from the transmitted line) are detected at 2.21 GHz and 2.29 GHz. Directly after the FPCs the suppression of strongest modes are 78 dB and 76 dB respectively with an uncertainty of 1 dB. The measured suppression thus agrees with the estimation calculated from the FPC's finesse. The SHG stage decreases the suppression by 6 dB (in accordance with theory), resulting in a suppression of 72 dB and 70 dB in front of the PCF. After sending the light through the PCF the suppression of the same intermediate modes is still 56 dB and 55 dB, respectively (see figure S4). Thus, our setup with three FPCs is sufficient to allow for an accuracy of the LFC calibration below the 1 cm s^{-1}-level.

Coupling the frequency comb to HARPS

The light of our frequency comb system was coupled to HARPS via those fibers, which in normal operation are used to deliver the calibration light of

the thorium lamp to the spectrograph. After the PCF the comb light was coupled to a multimode fiber (F1, 1 mm core diameter). Either a collimating lens is used to focus the light directly onto the fiber input facet or the fiber is attached to an integrating sphere that is fed with the comb light. In the F1 fiber the light is guided to the calibration unit of HARPS. This is a rack, in which several lamps are installed, e.g. thorium lamps for calibration or white-light sources for taking pixel sensitivity maps (flat fields). At the calibration unit, optics with a 10:1 demagnification are installed that are designed to focus the light of two lamps onto two fibers (F2, 300 μm core diameter), bringing the calibration light to the telescope's focal plane (TFP). The same optics were used to couple the comb light from F1 to F2, projecting the comb light onto a 100 μm spot on the input facet of the F2 fibers. Each of these then projects a spot of 750 μm diameter on the TFP. The projected light is collected by one or both of the two fibers (F3, 70 μm core diameter) that bring the light to the spectrograph. At the TFP, light from each of the F2 fibers or starlight from the telescope can be coupled to any of the F3 fibers. The images of the two fibers on the CCD are termed channel A and B respectively. In the path to the spectrograph, a static optical scrambler exchanges the F3 fibers' near-field and far-field to reduce the effect of an inhomogeneous illumination of the input facet of F3. For our calibration tests, a dynamic scrambler was attached to F1 which actively shook the fiber to increase the occupancy of spatial modes in the fiber [8].

Data reduction

A plot of the raw data from part of the two CCD chips is shown in figure 1A of the main text. These files are processed with the standard HARPS data reduction routine to obtain one-dimensional spectra. First, the count rate originating from the readout electronics (termed "bias") is subtracted from the data. In a second step, the dark count rate during an exposure and the event rate of cosmic rays hitting the detector are corrected for. Next, pixel-to-pixel sensitivity variations (encoded in a "flat field") as well as the overall efficiency curve of the individual orders (its "blaze") are determined by evaluating an illumination with a white light source. The geometric form of the orders on the CCD is then determined from the same white-light illumination and a fourth order polynomial is derived for each order to describe its center position along the chip. The one-dimensional spectrum is extracted

using the algorithm developed by Horne [29] and finally it is divided by the flat field.

The dispersion on the CCD is roughly 1.6 GHz per pixel, corresponding to about one third of the resolution. A single comb line is therefore projected onto ~ 3 pixels (FWHM) with a spatial distribution given by the instrumental profile (IP) of the spectrograph plus the input aperture. The center of the line and an estimate of its uncertainty can be derived from a fit to the data. The fit function should ideally be the IP, but this is not exactly known and also cannot be easily derived, as it is not constant throughout the whole spectrum. A Gaussian is a good approximation of the IP and is thus chosen as fit function. Note that systematic effects due to projection and fitting are common mode for differential measurements and cancel to a high degree.

The repeatability of the calibration is determined by taking a long series of subsequent acquisitions and computing the standard deviation of the average drift of the acquisitions with respect to a reference acquisition. The reference acquisition is arbitrarily chosen and the difference between each line in the acquisition of interest and the reference is computed in pixel units. According to the known frequency of each line, the pixel difference is converted into a shift in units of radial velocity. The average shift of all lines in the acquisition of interest is computed, weighted with the uncertainties associated with the fitted line positions. The scatter of these average drifts during a series of acquisitions, measured by the standard deviation, gives the calibration repeatability. The algorithm to compute the LFC's calibration repeatability from the one-dimensional spectra was developed specifically for this study.

The spectrum we generated has the potential for a photon noise limit of $2\,\mathrm{cm\,s^{-1}}$ in a single acquisition, provided that the spectrum will be flattened in intensity at -20 dB below the peak. This has not yet been developed until our measurement campaign and thus the photon noise in one acquisition is generally around $6\,\mathrm{cm\,s^{-1}}$. However, by adding the photoelectrons of consecutive acquisitions before computing the drift, the number of accumulated photons can be increased and the photon noise limit is lowered.

A measure to quantify the stability of an observable — in this case the average line position — over time is the Allan deviation. Originally, it was introduced to measure the frequency stability of an oscillator, e.g. an atomic clock [19]. The Allan deviation $\sigma_y(\tau)$ is defined as the square root of the average quadratic difference of two subsequent measurements of an observable y (originally the oscillator's phase) after a time interval τ

$$\sigma_y(\tau) = \sqrt{\frac{1}{2}\langle (y_k - y_{k+1})^2 \rangle} \tag{2}$$

where $\langle\ \rangle$ denotes an infinite time average and there is no dead-time between the measurement of y_k and y_{k+1}. As usual, the Allan deviation is the square root of the Allan variance. A generalized version of the Allan deviation is the 2-sample deviation which allows for a dead-time between two subsequent measurements as it is the case for the spectrograph calibration data due to the read-out time. When no change to the comb's intensity is made during one series the 2-sample deviation can be plotted versus the accumulated number of photons instead of the acquisition time. In this way, series with different intensity are easily compared, because the number of accumulated photons uniquely determines the photon noise limit (See figure 3 of the main text).

Investigation of systematic effects

While the short-term calibration of the HARPS spectrograph with our frequency comb is photon noise limited, the long-term calibration clearly is not. Especially the two series in which an integrating sphere (IS) is employed show a strong deviation in the differential drift between the two channels. This can give a hint at the dominant systematics. There are three major effects of the IS: The intensity is reduced by several orders of magnitude (which can be compensated to a reduction of only one order of magnitude by increasing the flux from the LFC and the exposure time), the spatial modes of the multimode fiber at the output are occupied homogeneously, and the polarization of the beam is randomized. Series without the IS, in which the polarization of the beam entering the multimode fiber is varied, show no effect on the differential drift. The other two effects, however, need to be investigated in further detail. While the occupation of the spatial modes in the multimode fiber directly affects the position of the line on the detector, a reduced SNR can induce a line shift if the line shape is asymmetric. What we consider at present the most likely origins of the systematic line shifts is discussed in the following.

Asymmetric instrumental profile Monochromatic light is imaged onto the detector of HARPS with a distribution that defines the IP. The IP is not centrosymmetric but has a slight asymmetry after the extraction of the

one-dimensional spectrum. Fitting a symmetric model function (such as a Gaussian) to the IP will give the same center position independent of the signal level, as long as there is no background noise. Assuming that there is a constant background noise, however, a reduction of the line's signal level will induce a shift of the measured line center when fitting a symmetric function to the line. To some extent, our evaluation is prone to this effect since the true IP is unknown and surely not perfectly symmetric. Efforts to model the IP have been made but thus far the observed systematic line shifts could not be explained by assuming a simple analytic model of an asymmetric IP in combination with a varying SNR. If the systematic shifts in our data cannot be explained by other effects, the IP should be measured precisely — e.g. by use of the LFC with its unresolved and tunable lines — to calibrate this effect.

Charge transfer inefficiency Even if the image of a monochromatic beam on the detector were symmetric the read-out process of the detector will induce an asymmetry. When the electrons are shuffled from one pixel to the next during read-out this transfer is not perfect and a fraction of the charge remains in the original pixel. This effect is termed charge transfer inefficiency (CTI). An important characteristic is that it is dependent on the signal level [30]. Typically, for high signal levels the CTI is almost constant (better than 10^{-6} for HARPS) but it increases with decreasing signal. Therefore, CTI will lead to a signal-dependent deformation of an initially symmetric line and thus to a signal-dependent shift of the line center. Recently, this effect was characterized in detail for the SOPHIE spectrograph at the Observatoire de Haute Provence and correction factors could be determined for that spectrograph [31]. The effect is supposedly much smaller with the HARPS detector but its characterization should also be performed for HARPS and might possibly remove the dominant systematic line shift.

Light injection The variation of the light injection into the multimode fiber is known to have an effect on the line positions on the detector [8]. The comb light coming out of the PCF is an almost perfect fundamental Gaussian beam. When coupling this beam into a multimode fiber via a collimating lens, only few of the spatial modes in the fiber are occupied. A mode scrambler will increase the occupancy and reduce the sensitivity to the injection. For this reason, a dynamic scrambler is employed at the first multimode fiber. The

dynamic scrambler is sufficient to reduce the sensitivity to the beam injection below the photon noise in series during which the system is untouched. It might, however, be insufficient if the injection is changed strongly between the series. Since the IS is changing the injection from minimum mode occupancy (without the IS) to a very high occupancy, this might explain why the series with the IS are shifted so strongly from the other series. A careful analysis of the impact of the light injection on the line shift is necessary to determine whether this is the limiting systematic effect.

Observations of the planet-host star HD75289

The star HD75289 is an inactive, 6 Gyr old dwarf star, in the constellation of Vela. Its mass and luminosity are slightly larger than solar, and it belongs to the G0 spectral class. In the year 2000, an orbiting planet was detected via the radial velocity method using the CORALIE spectrograph installed at the Euler Swiss telescope in La Silla Observatory in Chile [21]. As for other stars hosting giant planets in tight orbits, HD75289 is more rich in metal than the Sun. The planet has a period of 3.51 days, a projected mass $m \sin(i)$ of 0.4 times the mass of Jupiter, and zero eccentricity. Orbiting at a distance of 0.046 AU from its parent star, it belongs to the class of "hot jupiters" giant planets strongly irradiated by their star.

During our observing campaign we have collected eight radial velocity measurements of this star, obtained both with the LFC and with the thorium calibrations. The radial velocity data obtained with both calibrations are shown in table S1. We used three more data points in the HARPS archive to fit an orbit to the entire set of radial velocity data in our possession. The root mean square of the residuals around the keplerian fit is of $6.1\,\mathrm{m\,s^{-1}}$ for the thorium calibrated data and of $5.8\,\mathrm{m\,s^{-1}}$ for the LFC calibrated data, indicating that the two measurements are consistent, although the LFC data seem to have residuals which are marginally smaller than the thorium data. We expect that the measured residuals originate mostly from stellar activity or from a possible other body orbiting the star, and not from the calibration source.

This is the first time that the orbit of a planetary companion to a star has been reconstructed thanks to an LFC calibration of a spectrograph.

BJD	RV_{LFC}(m/s)	δRV_{LFC}(m/s)	RV_{Th}(m/s)	δRV_{Th}(m/s)
2455525.781	9305.71	0.47	9301.27	0.47
2455526.833	9339.04	0.55	9336.38	0.55
2455526.845	9343.02	0.50	9340.45	0.50
2455527.736	9408.06	0.51	9405.32	0.51
2455527.747	9408.40	0.51	9405.60	0.51
2455528.874	9337.47	0.45	9335.41	0.45
2455529.865	9308.03	0.82	9306.33	0.82
2455529.877	9312.12	0.64	9310.45	0.64

Table S1: Radial velocity (RV) data of the star HD75289 calibrated with the LFC and a thorium lamp (Th). The absolute RV determined with both calibrations are given together with the uncertainties δRV and the date of recording in Barycentric Julian Date (BJD). The uncertainties are dominated by the photon noise of the star data.

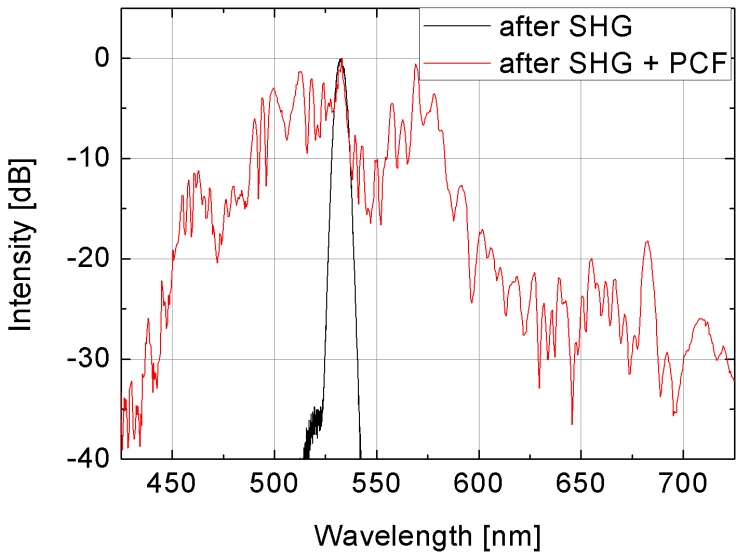

Figure S1: Typical spectral envelope of our frequency comb system before (black) and after (red) the PCF. After the SHG stage, 90 mW at a line spacing of 18 GHz (giving 5 pJ pulse energy) suffice to achieve spectral broadening of the initially 5 nm wide spectrum (full-width half-maximum) to more than 140 nm bandwidth at 20 dB below the peak.

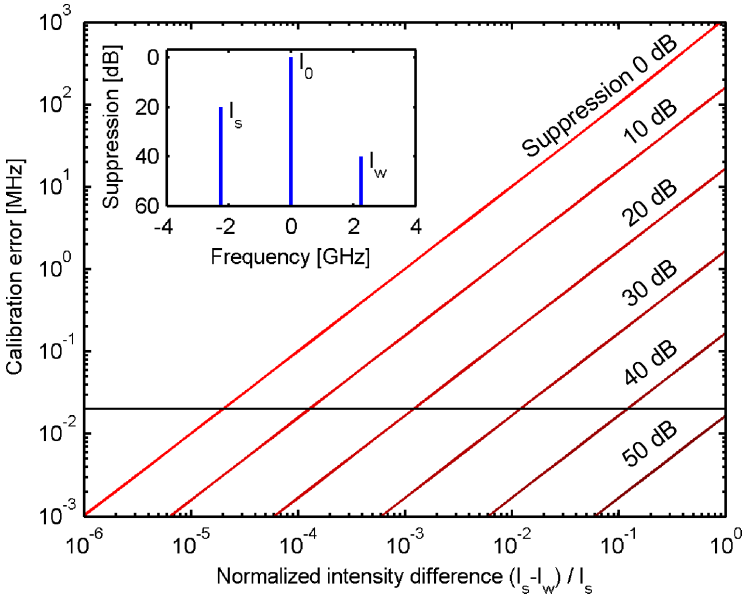

Figure S 2: Simulated calibration error of asymmetrically suppressed lines — as detected by a spectrograph — as a function of the asymmetry for various suppressions. The suppression is defined as the intensity ratio I_0/I_s between the transmitted line and the stronger of the neighboring lines. The separation between the lines is 2.25 GHz with an additional asymmetry between the suppressed lines (see inset). The spectrograph is assumed to have a Gaussian instrumental profile with a FWHM of 5 GHz (i.e. the neighboring lines are not resolved by the spectrograph). A normalized intensity difference of 10^0 corresponds to $I_w = 0$, i.e. the weaker neighboring line is completely suppressed. The black line indicates a calibration error of 20 kHz, corresponding to 1 cm s^{-1} radial velocity variation at 500 nm.

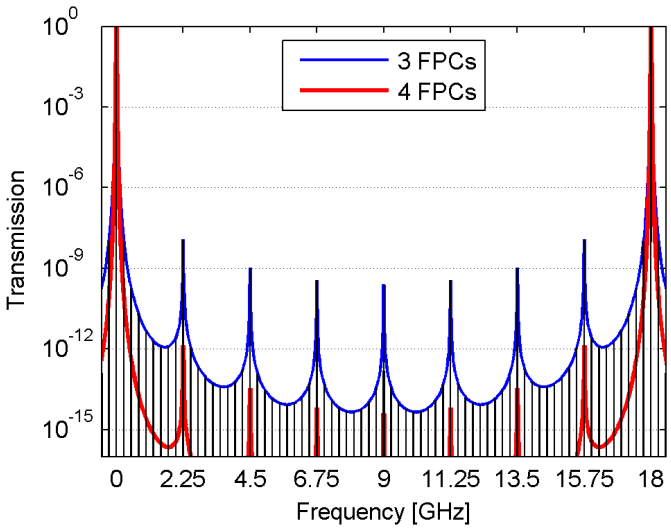

Figure S3: Simulated intensity distribution of the comb lines after the FPCs. The transmission is simulated for FPCs with a Finesse of $\mathcal{F} = 390$. The first FPC has a FSR of 2.25 GHz while all subsequent cavities have a FSR of 18 GHz. For a setup with three FPCs the strongest suppressed line is at 2.25 GHz from the transmitted line and its suppression is 79 dB. With four FPCs the strongest suppressed line is at 250 MHz with a suppression of 101 dB.

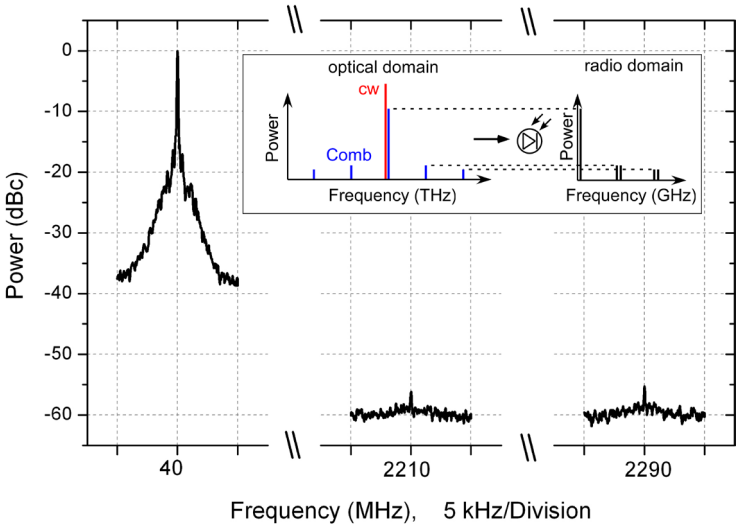

Figure S4: Measured intermediate mode suppression after the spectral broadening. A cw laser at 1065 nm is locked with an offset of 20 MHz to an LFC mode that is transmitted through the three FPCs. Both cw laser and LFC are frequency doubled. After broadening the LFC spectrum in a PCF the heterodyne beatnotes between cw laser and the LFC modes are detected on a photodiode (see insert). Due to frequency doubling the beatnote between the cw laser and the next transmitted LFC mode is at 40 MHz. Its power is normalized to 0 dBc. The strongest suppressed modes of the LFC are at ± 2.25 GHz from the transmitted mode. The beatnotes between those modes and the cw laser have a suppression of 55 dB and 56 dB, respectively, which equals the suppression of the intermediate LFC modes with respect to the transmitted mode. The resolution bandwidth is 91 Hz and 100 acquisitions have been averaged within $\sim$10 s which is the shortest acquisition time that has been used in the calibration tests at HARPS.

Additional References

[25] Pepe F., Mayor M., Rupprech G., "HARPS: ESOs Coming Planet Searcher" *The Messenger* **110**, 9 (2002).

[26] McFerran, J. J., "Echelle spectrograph calibration with a frequency comb based on a harmonically mode-locked fiber laser: a proposal" *Appl. Opt.* **48**, 2752 (2009).

[27] Del Haye, P. *et al.*, "Optical frequency comb generation from a monolithic microresonator" *Nature* **450**, 1214 (2007).

[28] Hartl, I. *et al.*, "GHz Yb-femtosecond-fiber laser frequency comb" *Conference on Lasers and Electro-Optics*, CMN1 (2009).

[29] Horne, K., "An optimal extraction algorithm for CCD spectroscopy", *Publ. Astron. Soc. Pac.* **98**, 609 (1986).

[30] Goudfrooij, P. *et al.*, "Empirical Corrections for Charge Transfer Inefficiency and Associated Centroid Shifts for STIS CCD Observations" *Publ. Astron. Soc. Pac.* **118**, 1455-1473 (2006).

[31] Bouchy, F. *et al.*, "Charge Transfer Inefficiency effect for high-precision radial velocity measurements" *EAS Publication Series* **37**, 247-253 (2009).